Python results: Hamaker coefficients for perpendicular [6,5] (semi-conductor) cylinders in water using retarded formulation.

JC Hopkins

May 13, 2014

Abstract

Comparison of contributions of Matsubara sums to the retarded formulation for
Hamaker coeffiecient, $\mathcal{A}^{(0)}$. I choose to use [6,5], a semiiconductor, and [9,3], a semimetal, as examples. All caluclations are for identical pairs of
CNTs in water with a mutual angle of $\pi/2$.

Equations correspond to those in version 4 of Rudi's report.

Contents

1 CNT Semi-conductor [6,5]

1.1 [6,5] Dielectric response spectrum, dispersion spectrum, and anisotropy measure

From the imaginary part of the dielectric response function of the carbon nanotubes,
we compute the London dispersion spectrum by the Kramers-Kronig transform:

$$\epsilon(i\zeta_n) = 1 + \frac{\pi}{2}\int_0^\infty dw\ \frac{\epsilon''(\omega)\omega}{\omega^2+\zeta^2} \tag{1}$$

Relative anisotropy measures in the parallel and perpendicular direction are given by

$$\Delta_\perp = \frac{{\epsilon^c}_\perp - \epsilon_m}{{\epsilon^c}_\perp + \epsilon_m} \qquad \Delta_\parallel = \frac{{\epsilon^c}_\parallel - \epsilon_m}{\epsilon_m}. \tag{2}$$

Ratio of anisotropy measure:

$$a_{1,2}(i\omega_n) = \frac{2\Delta_\perp^{(1,2)}(i\omega_n)}{\Delta_\parallel^{(1,2)}(i\omega_n)} = 2\frac{({\epsilon^c}_\perp{}^{(1,2)}(i\omega_n) - \epsilon_m(i\omega_n))\epsilon_m(i\omega_n)}{({\epsilon^c}_\perp{}^{(1,2)}(i\omega_n) + \epsilon_m(i\omega_n))({\epsilon^c}_\parallel{}^{(1,2)}(i\omega_n) - \epsilon_m(i\omega_n))} \tag{3}$$

For interactions between identical CNTs, we set $a_1 = a_2$.

1.2 [6,5] Dielectric contrast, anisotropy measure, and their derivatives

The relative anisotropy compares the dielectric contrasts, Δ, of the radial and axial responses of the CNTs in water.

For interactions between identical CNTs, we set $a_1 = a_2$.

The ratio of anisotropy measure is given as

$$a_{1,2}(i\omega_n) = \frac{2\Delta_\perp^{(1,2)}(i\omega_n)}{\Delta_\parallel^{(1,2)}(i\omega_n)} = 2\frac{({\epsilon^c}_\perp{}^{(1,2)}(i\omega_n) - \epsilon_m(i\omega_n))\epsilon_m(i\omega_n)}{({\epsilon^c}_\perp{}^{(1,2)}(i\omega_n) + \epsilon_m(i\omega_n))({\epsilon^c}_\parallel{}^{(1,2)}(i\omega_n) - \epsilon_m(i\omega_n))} \tag{4}$$

where the dielectric contrasts are given by

$$\Delta_\perp = \frac{{\epsilon^c}_\perp - \epsilon_m}{{\epsilon^c}_\perp + \epsilon_m} \qquad \Delta_\parallel = \frac{{\epsilon^c}_\parallel - \epsilon_m}{\epsilon_m}. \tag{5}$$

For the sake of completeness, I have plotted the behaviors of Δ and $a(i\zeta)$ as they appear in the equations for Hamaker Coefficients as well as their derivatives with respect to n.

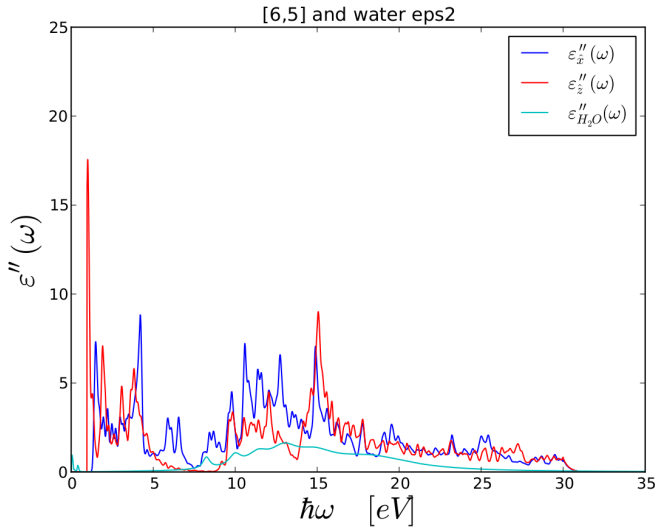

Figure 1: Imaginary dielectric response spectra for water and the axial and radial responses of anisotropic [6,5] CNTs

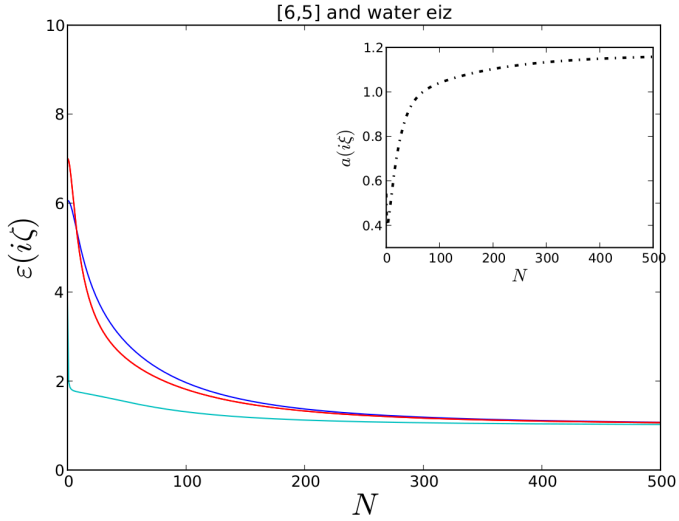

Figure 2: Dispersion spectrum for anisotropic [6,5] CNT's and water. The anisotropy measure, $a(i\zeta_n)$, is shown in the inset.

1.3 [6,5] Fully retarded Hamaker Coefficients for Matsubara Sum

Using equations from v.4 of Rudi's report, we calculate the fully retarded Hamaker coefficients for perpendicular, identical [6,5] CNTs in water, as given

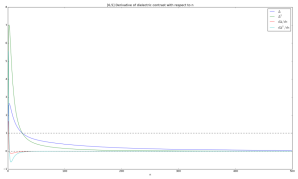

Figure 3: Dielectric contrast of [6,5] CNTs in water, its square, and their derivatives with respect to n.

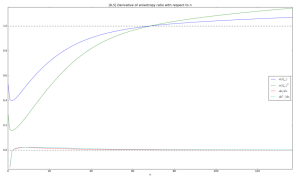

Figure 4: Anisotropy ratio of [6,5] CNTs in water, its square, and their derivatives with respect to n.

by:

$$\mathcal{A}^{(0)}(\ell) = \frac{k_B T}{32} {\sum_{n=0}^{\infty}}' \Delta_{1,\parallel}\Delta_{2,\parallel}\, p_n^4(\ell) \int_0^\infty t dt\, \frac{e^{-2p_n(\ell)\sqrt{t^2+1}}}{(t^2+1)} \tilde{g}^{(0)}(t, a_1(i\omega_n), a_2(i\omega_n)) \tag{6}$$

$$\tilde{g}^{(0)}(t, a_1(i\omega_n), a_2(i\omega_n)) = 2\left[(1+3a_1)(1+3a_2)t^4 + 2(1+2a_1+2a_2+3a_1a_2)t^2 + 2(1+a_1)(1+a_2)\right]$$

and

$$\mathcal{A}^{(2)}(\ell) = \frac{k_B T}{32} {\sum_{n=0}^{\infty}}' \Delta_{1,\parallel}\Delta_{2,\parallel}\, p_n^4(\ell) \int_0^\infty t dt\, \frac{e^{-2p_n(\ell)\sqrt{t^2+1}}}{(t^2+1)} \tilde{g}^{(2)}(t, a_1(i\omega_n), a_2(i\omega_n), \theta) \tag{7}$$

$$\tilde{g}^{(2)}(t, a_1(i\omega_n), a_2(i\omega_n), \theta) = (1 - a_1)(1 - a_2)(t^2 + 2)^2 \tag{8}$$

with the n = 0 term given by

$$\mathcal{A}^{(0)}_{n=0}(\ell) = \frac{1}{2}\frac{k_B T}{32}\Delta_{1,\parallel}\Delta_{2,\parallel} \int_0^\infty u^3 du\ e^{-2u}\ [2(1 + 3a_1)(1 + 3a_2)] \tag{9}$$

and

$$\mathcal{A}^{(2)}_{n=0}(\ell) = \frac{1}{2}\frac{k_B T}{32}\Delta_{1,\parallel}\Delta_{2,\parallel} \int_0^\infty u^3 du\ e^{-2u}\ [(1 - a_1)(1 - a_2)] \tag{10}$$

where $u = Ql$.

The two figures below give the fully retared Hamaker coefficents,
$\mathcal{A}^{(0)}$ and $\mathcal{A}^{(2)}$, as a function of separation.

Log-log plot of Hamaker coeffcients as a function of separation:

Semi-log plot of Hamaker coeffcients as a function of separation:

1.4 [6,5] Terms of Matsubara sum and their derivatives with respect to ℓ and n

We investigate the amount that each term contributes to the Matsubara sum, in
the Hamaker coefficents, $\mathcal{A}^{(0)}$ and $\mathcal{A}^{(2)}$.

$$\mathcal{A}^{(0)}(\ell) = \frac{k_B T}{32}{\sum_{n=0}^{\infty}}' \Delta_{1,\parallel}\Delta_{2,\parallel}\, p_n^4(\ell) \int_0^\infty t dt\ \frac{e^{-2p_n(\ell)\sqrt{t^2+1}}}{(t^2+1)}\tilde{g}^{(0)}(t, a_1(i\omega_n), a_2(i\omega_n)) \tag{11}$$

and

$$\mathcal{A}^{(2)}(\ell) = \frac{k_B T}{32}{\sum_{n=0}^{\infty}}' \Delta_{1,\parallel}\Delta_{2,\parallel}\, p_n^4(\ell) \int_0^\infty t dt\ \frac{e^{-2p_n(\ell)\sqrt{t^2+1}}}{(t^2+1)}\tilde{g}^{(2)}(t, a_1(i\omega_n), a_2(i\omega_n), \theta) \tag{12}$$

with the n = 0 term given by

$$\mathcal{A}^{(0)}_{n=0}(\ell) = \frac{1}{2}\frac{k_B T}{32}\Delta_{1,\parallel}\Delta_{2,\parallel} \int_0^\infty u^3 du\ e^{-2u}\ [2(1 + 3a_1)(1 + 3a_2)] \tag{13}$$

and

$$\mathcal{A}^{(2)}_{n=0}(\ell) = \frac{1}{2}\frac{k_B T}{32}\Delta_{1,\parallel}\Delta_{2,\parallel} \int_0^\infty u^3 du\ e^{-2u}\ [(1 - a_1)(1 - a_2)] \tag{14}$$

where $u = Ql$.

The following plot shows the value of each term of $\mathcal{A}$ for different values of separations. As separations increase,
more of the higher frenquency terms of $\mathcal{A}^{(0)}$ show a weakened contribution to the sum.

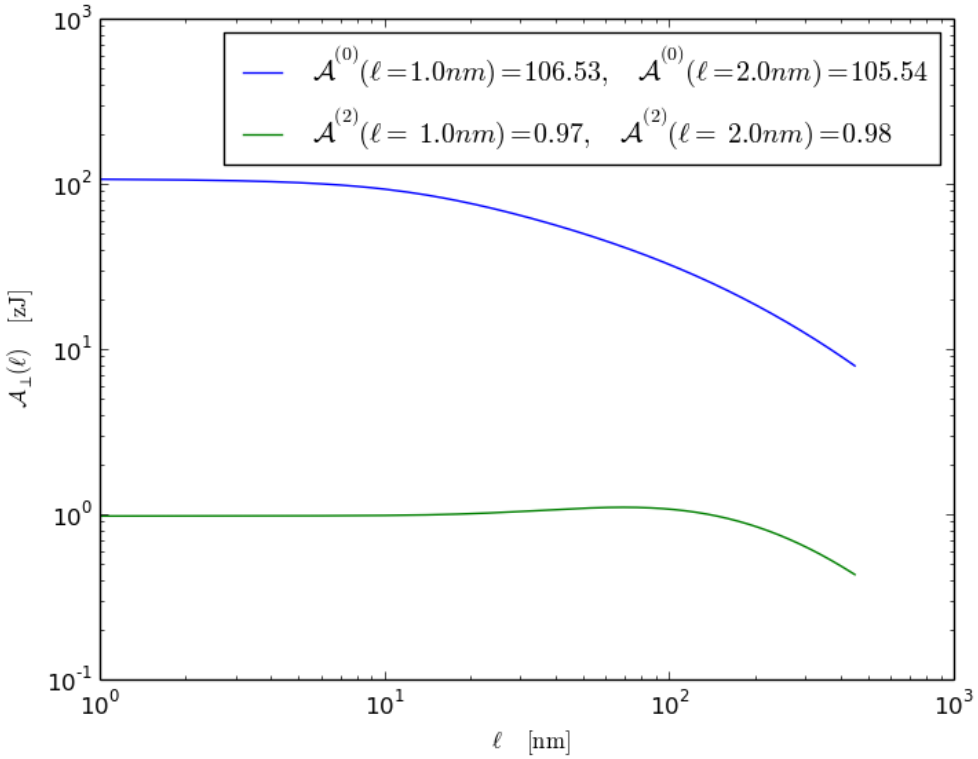

Figure 5: Log-log plot of fully retarded Hamaker coeffiecents for perpendicular, identical [6,5] CNT's in water as a function of separation.

2 Finite c effect: change in contributions to Matsubara sum of $\mathcal{A}^{(0)}$

2.1 [6,5] as an example of power law knee in $\mathcal{A}^{(0)}$ and inflection points in $d\mathcal{A}^{(0)}/d\ell$

$$\mathcal{A}^{(0)}(\ell) = \frac{k_B T}{32} {\sum_{n=0}^{\infty}}' \Delta_{1,\parallel}\Delta_{2,\parallel}\, p_n^4(\ell) \int_0^\infty t dt\, \frac{e^{-2p_n(\ell)\sqrt{t^2+1}}}{(t^2+1)} \tilde{g}^{(0)}(t, a_1(i\omega_n), a_2(i\omega_n)) \tag{15}$$

with

$$\tilde{g}^{(0)}(t, a_1(i\omega_n), a_2(i\omega_n)) = 2\left[(1+3a_1)(1+3a_2)t^4 + 2(1+2a_1+2a_2+3a_1a_2)t^2 + 2(1+a_1)(1+a_2)\right]$$

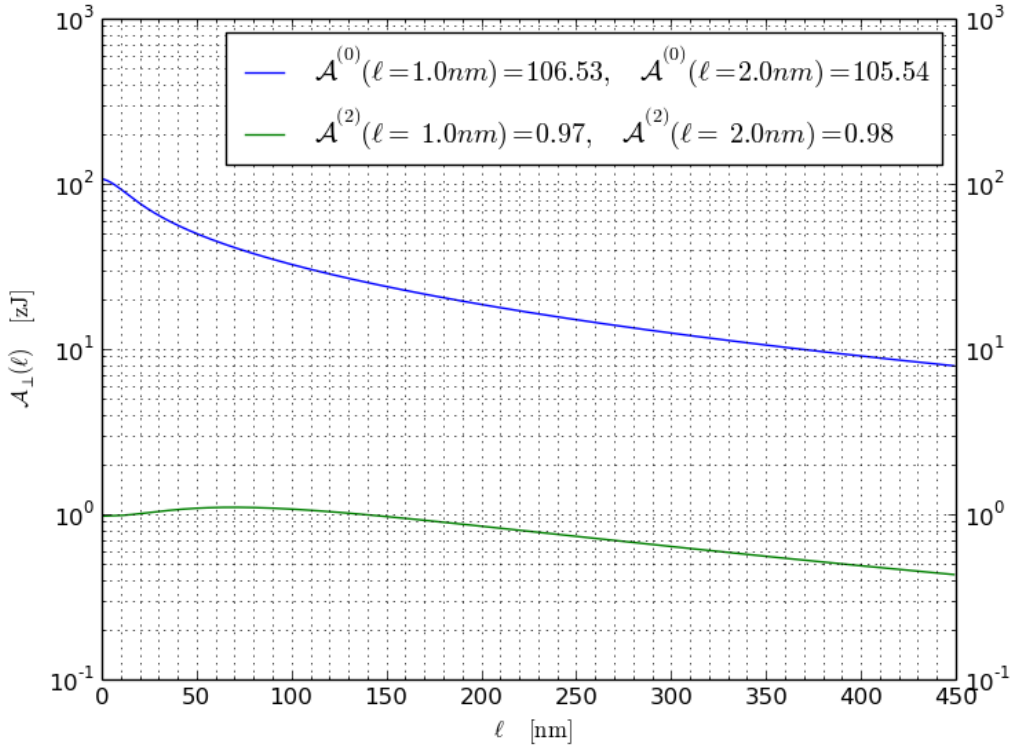

Figure 6: Semi-log plot of fully retarded Hamaker coeffiecents for perpendicular, identical [6,5] CNT's in water as a function of separation.

and

$$\mathcal{A}^{(2)}(\ell) = \frac{k_B T}{32} {\sum_{n=0}^{\infty}}' \Delta_{1,\parallel}\Delta_{2,\parallel}\, p_n^4(\ell) \int_0^\infty t dt\, \frac{e^{-2p_n(\ell)\sqrt{t^2+1}}}{(t^2+1)} \tilde{g}^{(2)}(t, a_1(i\omega_n), a_2(i\omega_n), \theta) \tag{16}$$

with

$$\tilde{g}^{(2)}(t, a_1(i\omega_n), a_2(i\omega_n), \theta) = (1-a_1)(1-a_2)(t^2+2)^2 \tag{17}$$

2.2 Ratio of signal travel time to flucuation lifetime

Round-trip distance between correlated charge fluctuations: 2ℓ// Round-trip travel time: $(2\ell)/(c/\sqrt{\epsilon_m})$ // Fluctuation lifetime = $1/\zeta_n$// Ratio r_n = travel time/flucuation lifetime = $2\ell\sqrt{\epsilon_m}\zeta_n/c = (1/2)p_n(\ell)$ from RP's report//

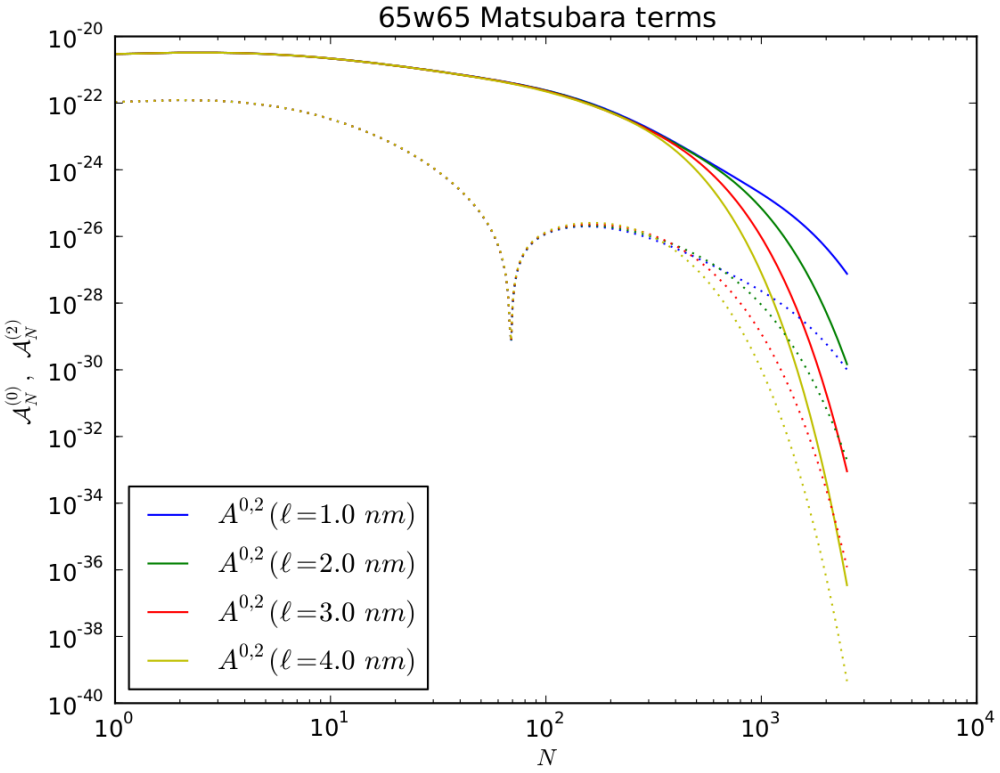

Figure 7: **Terms contributing to Matsubara sum as a function of n. The terms of $\mathcal{A}^{(2)}$ show a sharp valley at the value of n for which the dispersion spectra, $\epsilon_\perp$ and $\epsilon_\parallel$, have their closest approach to each other.**

$$\mathcal{A}^{(0)}(\ell) = \frac{k_B T}{32} {\sum_{n=0}^{\infty}}' \Delta_{1,\parallel}\Delta_{2,\parallel}\, p_n^4(\ell) \int_0^\infty t dt\, \frac{e^{-2p_n(\ell)\sqrt{t^2+1}}}{(t^2+1)} \tilde{g}^{(0)}(t, a_1(i\omega_n), a_2(i\omega_n)) \tag{18}$$

$$\tilde{g}^{(0)}(t, a_1(i\omega_n), a_2(i\omega_n)) = 2\left[(1+3a_1)(1+3a_2)t^4 + 2(1+2a_1+2a_2+3a_1a_2)t^2 + 2(1+a_1)(1+a_2)\right] \tag{19}$$

and

$$\mathcal{A}^{(2)}(\ell) = \frac{k_B T}{32} {\sum_{n=0}^{\infty}}' \Delta_{1,\parallel}\Delta_{2,\parallel}\, p_n^4(\ell) \int_0^\infty t dt\, \frac{e^{-2p_n(\ell)\sqrt{t^2+1}}}{(t^2+1)} \tilde{g}^{(2)}(t, a_1(i\omega_n), a_2(i\omega_n), \theta) \tag{20}$$

with

$$\tilde{g}^{(2)}(t, a_1(i\omega_n), a_2(i\omega_n), \theta) = (1-a_1)(1-a_2)(t^2+2)^2 \tag{21}$$

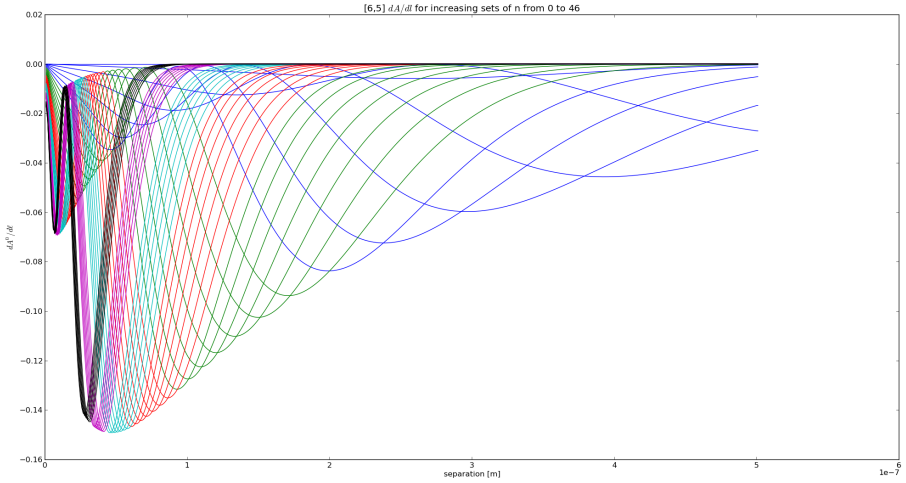

Figure 8: **The derivative of $\mathcal{A}^{(0)}$ with respect to separation for a range of values of n from n=0 to n=46.** Derivative of Matsubara terms with respect to ℓ, $d\mathcal{A}^{(0)}/d\ell$, for two perpendicular [6,5] CNTs in water. Colors represent groups of six increasing adjacent vales of n, i.e. for n=(0 to 6) blue, n = (10 to 16) green, n = (20 to 26) red, and so on to n = (40 to 46) black.

where $p_n^2(\ell) = \epsilon_m(i\omega_n)\frac{\omega_n^2}{c^2}\ell^2$.
with the n = 0 term given by

$$\mathcal{A}^{(0)}_{n=0}(\ell) = \frac{1}{2}\frac{k_BT}{32}\Delta_{1,\|}\Delta_{2,\|}\int_0^\infty u^3du\ e^{-2u}\ [2(1+3a_1)(1+3a_2)] \tag{22}$$

and

$$\mathcal{A}^{(2)}_{n=0}(\ell) = \frac{1}{2}\frac{k_BT}{32}\Delta_{1,\|}\Delta_{2,\|}\int_0^\infty u^3du\ e^{-2u}\ [(1-a_1)(1-a_2)] \tag{23}$$

where $u = Ql$.

where $p_n^2(\ell) = \epsilon_m(i\omega_n)\frac{\omega_n^2}{c^2}\ell^2$.

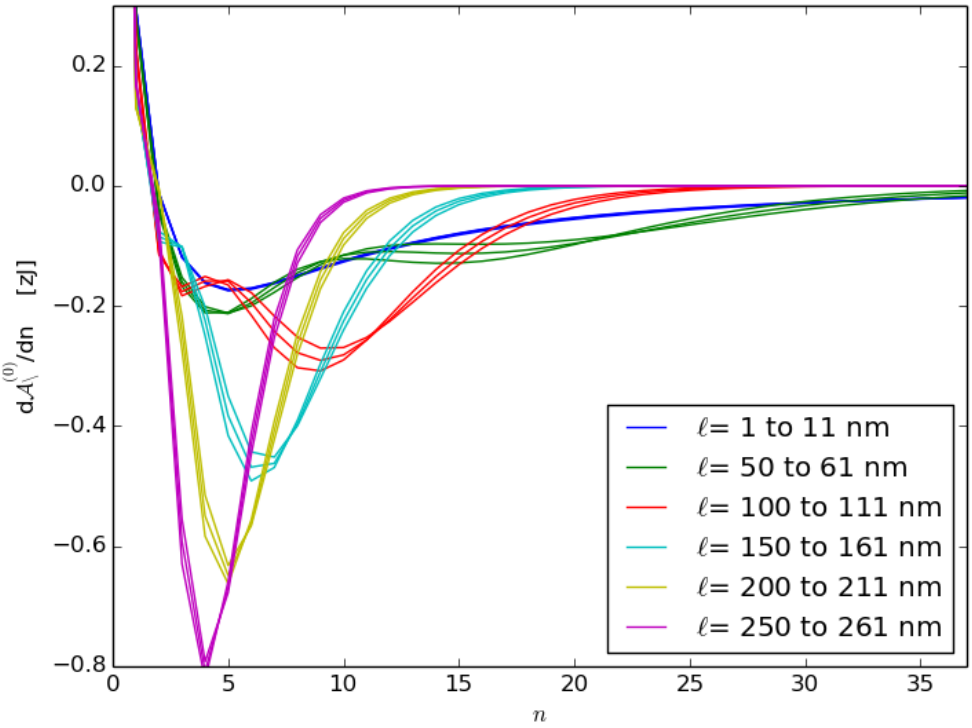

Figure 9: **The derivative of $\mathcal{A}^{(0)}$ with respect to n for different values of separation.** Derivative of Matsubara terms with respect to n, $d\mathcal{A}^{(0)}/dn$, for two perpendicular [6,5] CNTs in water. Colors represent groups of 3 values of ℓ, i.e. blue for ℓ= 1,6,11 nm, green for n = 50,56,61; red for ℓ = 100,106,111, and so on.

3 Comparison to Siber plots: in progress (the plots shown here need a correction to the n=0 terms)

3.1 [6,5] semi-conductor: retarded and non-retarded free energies

3.2 [9,3] semi-conductor: retarded and non-retarded free energies

4 Tables

Rajter's results were calculated using a water LDS with large peak at n=0, Int. J. Mat. Res 101 (2010). Gecko Hamaker and Python results use Dan's

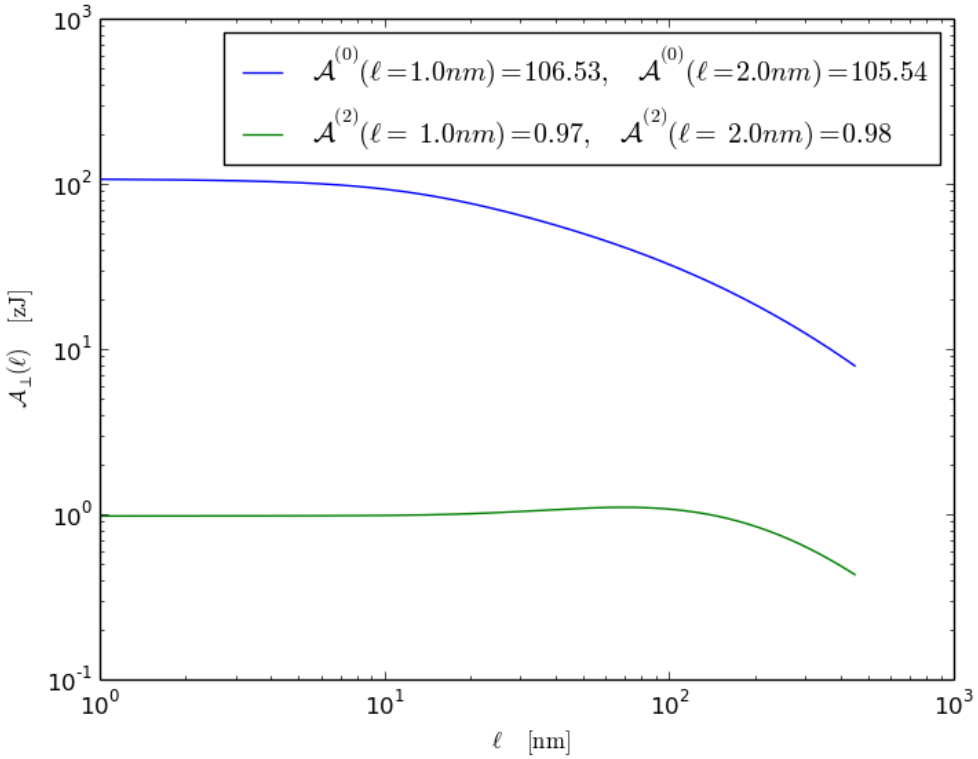

Figure 10: $\mathcal{A}^{(0,2)}$ **as a function of separation for identical [6,5] CNTs in water.** For some separation, ℓ, the function $\mathcal{A}^{(0)}$ displays a knee due to a changge in power law.

water spectrum.

4.1 Table of published results

4.2 Table of python results

*data from Chirality-dependent properties of carbon nanotubes: electronic structure, optical dispersion properties, Hamaker coefficients and van der WaalsLondon dispersion interactions Rick F. Rajter, Roger H. French, W.Y. Ching, Rudolf Podgornik and V. Adrian Parsegian RSC Adv., 2013,3, 823-842 DOI: 10.1039/C2RA20083J

4.3 Table of Gecko Hamaker results

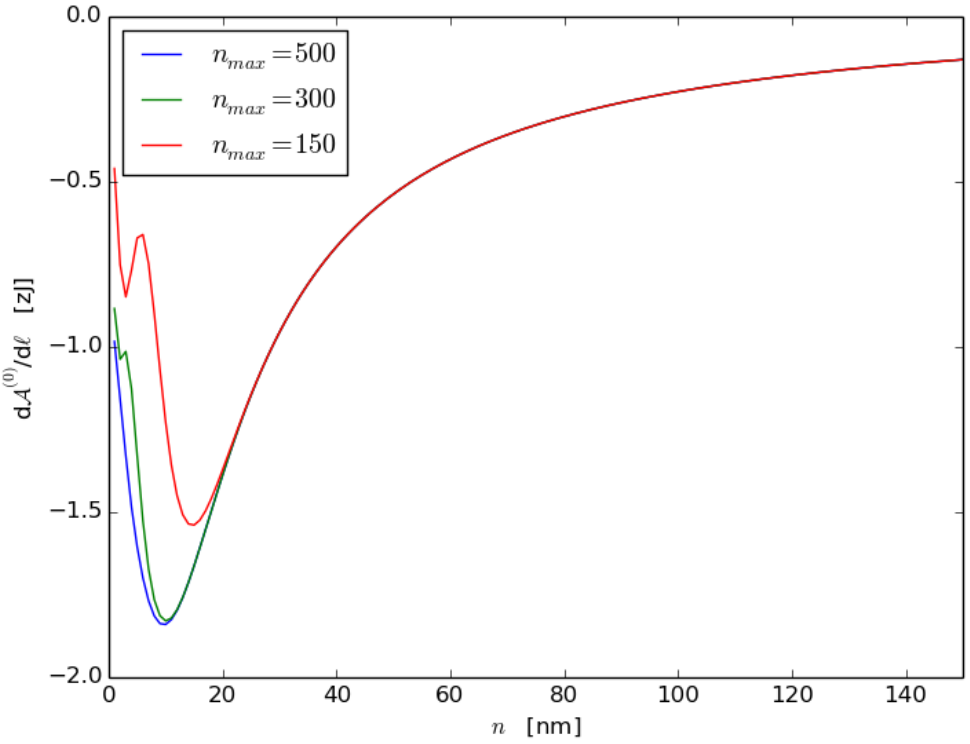

Figure 11: **Derivative of $\mathcal{A}^{(0)} = \sum \mathcal{A}_n^{(0)}$ as a function of separation for Matsubara sums to n=500,300, and 150.** For typical calculations of this type of CNT, sums from n=0 to n=500 are sufficient to capture n-dependant behavior and are accurate to about 0.01 percent of sums to n=10,000. I use an upper limit of n = 500 for my computations, shown in blue. A knee occurs in $\mathcal{A}^{(0)}(\ell)$ at the separation value for which $d\mathcal{A}^{(0)}/d\ell \approx 0$. However, some of my other calculations have indicated the existance of two inflection points at low values of n and ℓ in $\partial\mathcal{A}^{(0)}/\partial\ell$ as well as in $\partial\mathcal{A}^{(0)}/\partial n$. It appears that summing over the n's has the effect of blurring the two inflection points into one inflection point. The plot shows the derivative of $\mathcal{A}^{(0)}$ with respect to separation with n=500 (blue), n= 300 (green), and n=150 (red) used as the upper limit of the Matsubara sum. When higher values of n are removed from the sum, their effect of merging the two inflection points is also removed, as seen in green in red.

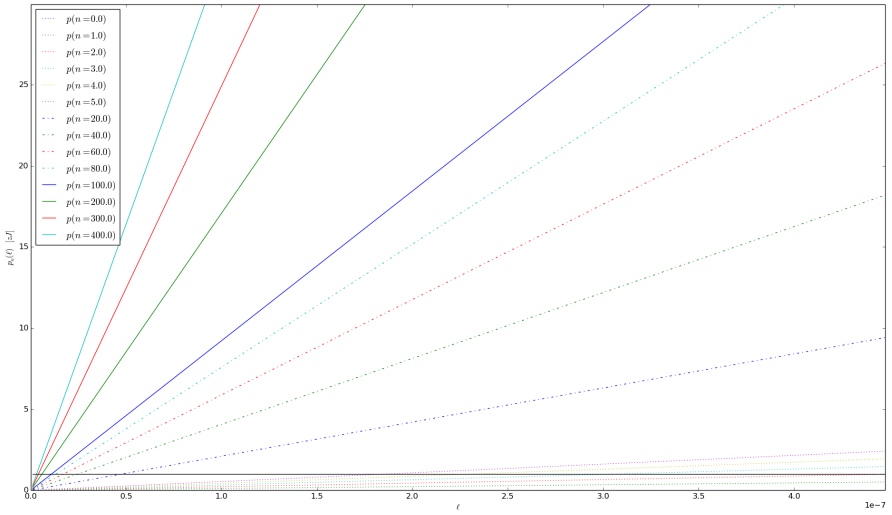

Figure 12: $p_n(\ell)$ **vs** ℓ for several values of n, where $p_n^2(\ell) = \epsilon_m(i\omega_n)\frac{\omega_n^2}{c^2}\ell^2$. . For each value of n (corresponding to different line colors and line styles), there is an ℓ value for which $p_n(\ell) = 1$. A black line is provided to show $p_n = 1$.

Table 1: Rajter results from IJMR perpendiuclar cylinders in water (Rajter's spectrum)

CNT	$\mathcal{A}^0$ [zJ]	$\mathcal{A}^2$ [zJ]
[6,5]	106	1.9
[9,0]	-	
[9,1]	92.8	3
[9,3]	107	36.2
[29,0]	18.5	0.8

Table 2: Python results, retarded formulation: perpendiuclar cylinders in water, intersurface distance = 1 nm

CNT	atoms*	radius*[A]	Type*	Geom*	$\mathcal{A}^{(0)}$(n=0) [zJ]	$\mathcal{A}^{(2)}$(n=0) [zJ]	$\mathcal{A}^{(0)}$ [zJ]	$\mathcal{A}^{(2)}$ [zJ]
[6,5]	364	3.734	sc	chiral	0.287	0.004	106.53	0.97
[9,0]	xxx	xxxxx	xx	xxxxxx	0.0	0.0	576.35	203.58
[9,1]	364	3.734	sc	chiral	0.419	0.010	94.50	1.57
[9,3]	156	4.234	sm	chiral	0.0	0.0	83.06	3.23
[29,0]	116	11.352	sc	zigzag	0.308	0.010	17.91	0.41

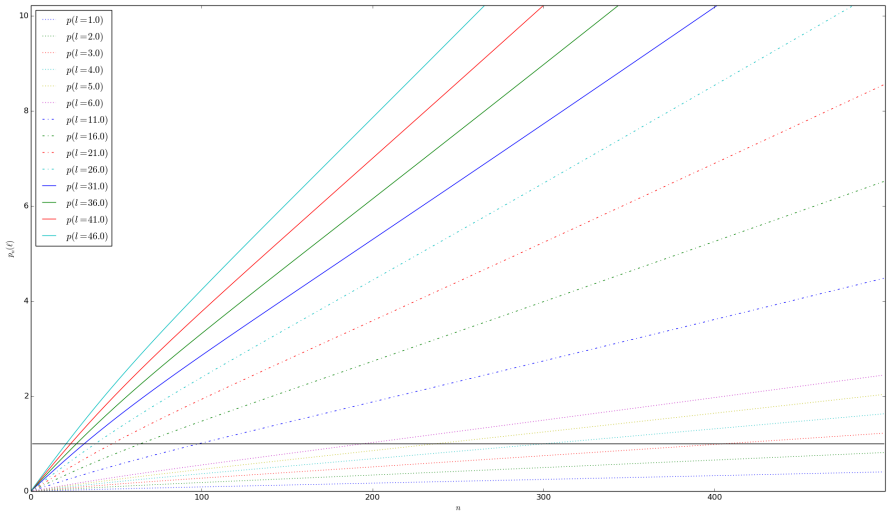

Figure 13: $p_n(\ell)$ **vs** n for several values of ℓ. For each value of ℓ (corresponding to different line colors and line styles), there is an n value for which $p_n(\ell) = 1$. A black line is provided to show $p_n = 1$.

Table 3: Python results, non-retarded formulation: perpendiuclar cylinders in water

CNT	$\mathcal{A}^0$ [zJ]	$\mathcal{A}^2$ [zJ]
[6,5]	126.80	1.16
[9,0]	semi-metal; in progress	
[9,1]	112.22	1.87
[9,3]	semi-metal; in progress	
[29,0]	20.93	0.49

Table 4: Gecko Hamaker results from 2.07, perpendiuclar cylinders in water

CNT	$\mathcal{A}^0$ [zJ]	$\mathcal{A}^2$ [zJ]
[6,5]	100	1.04
[9,0]	151	6.96
[9,1]	84.85	1.16
[9,3]	80.66	1.55
[29,0]	17.68	0.22

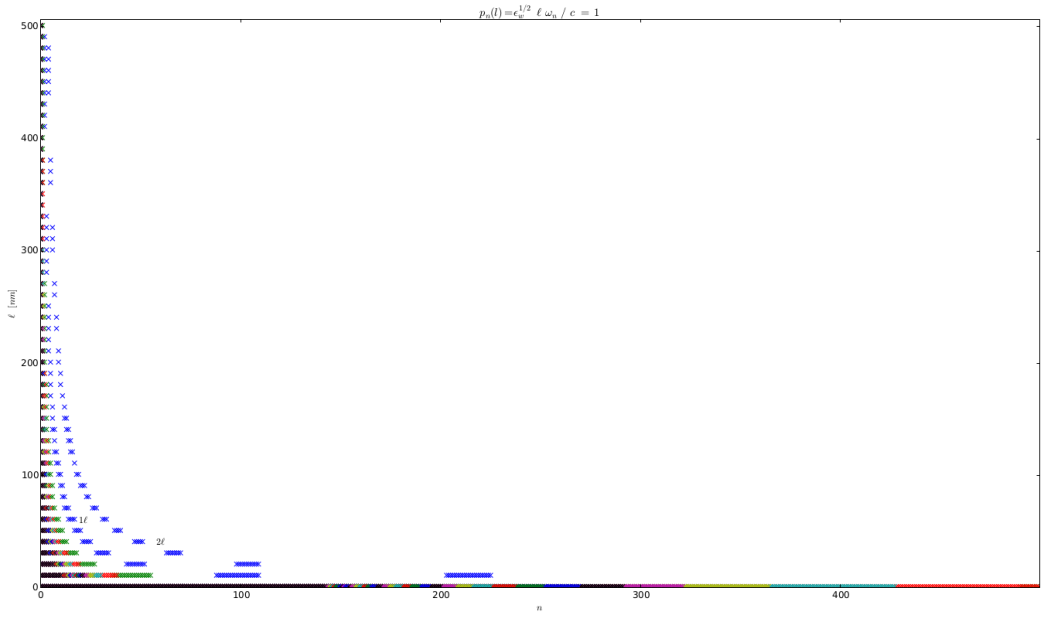

Figure 14: Plot of values of n,ℓ for which $p_n(\ell) = 1$. Blue stars with the label "1ℓ" are solutions to $p_n(\ell) = 1$ for travel time from $cylinder_1$ to $cylinder_2$, but not back to $cylinder_1$. Blue stars with the label "2ℓ" are solutions to $p_n(\ell) = 1$ for travel time from $cylinder_1$ to $cylinder_2$ and back to $cylinder_1$. Stars of other colors represent solutions to $p_n(\ell) < 1$.

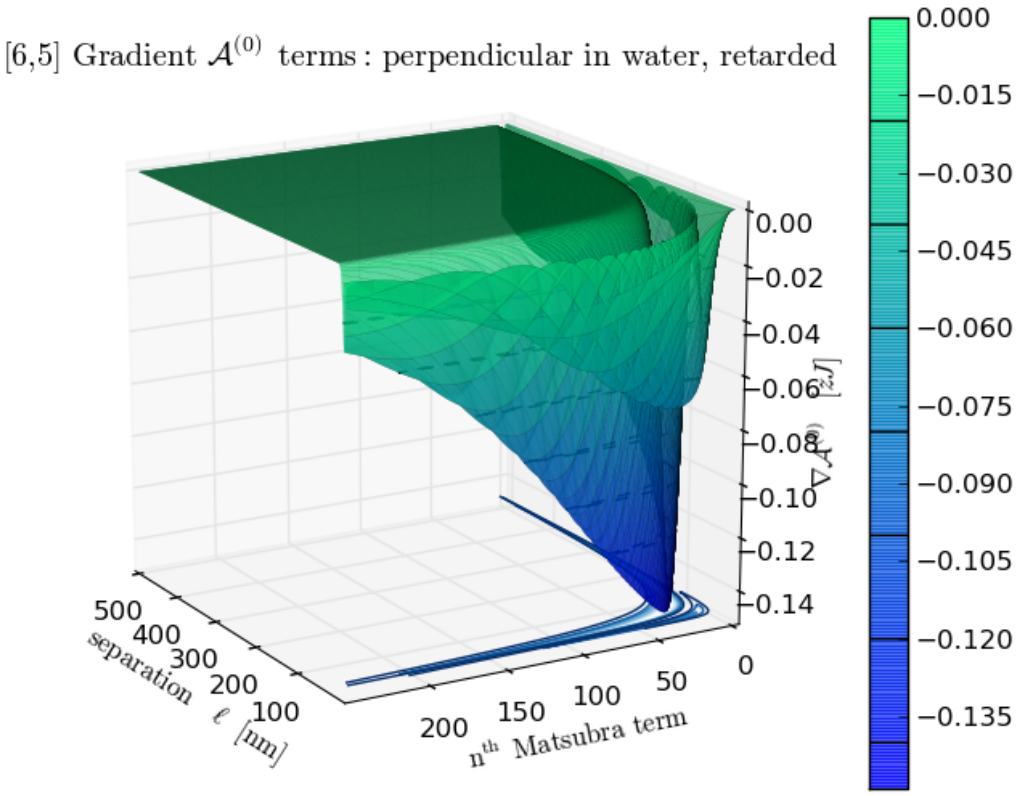

Figure 15: **Derivative of $\mathcal{A}_n^{(0)}(\ell))$ for [6,5] with resepct to n and separation.** Valleys in this 3D surface plot correspond to the infection points in $d\mathcal{A}^{(0)}/d\ell$ of fig. 11 of previous section and the solutions to $p_n(\ell) = 1$ in fig. 14 above.

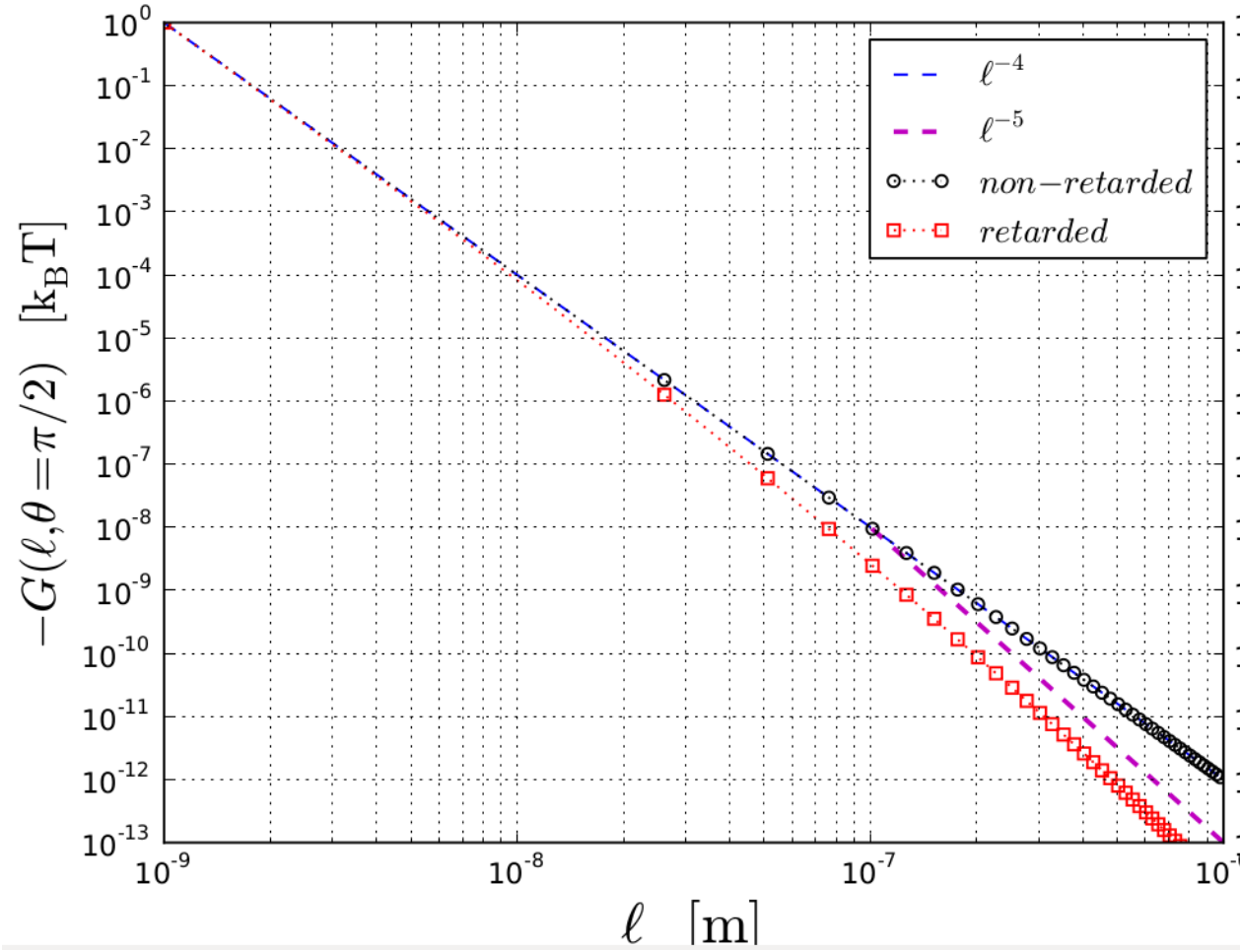

Figure 16: $\mathcal{G}(\ell)$ for [6,5] in water

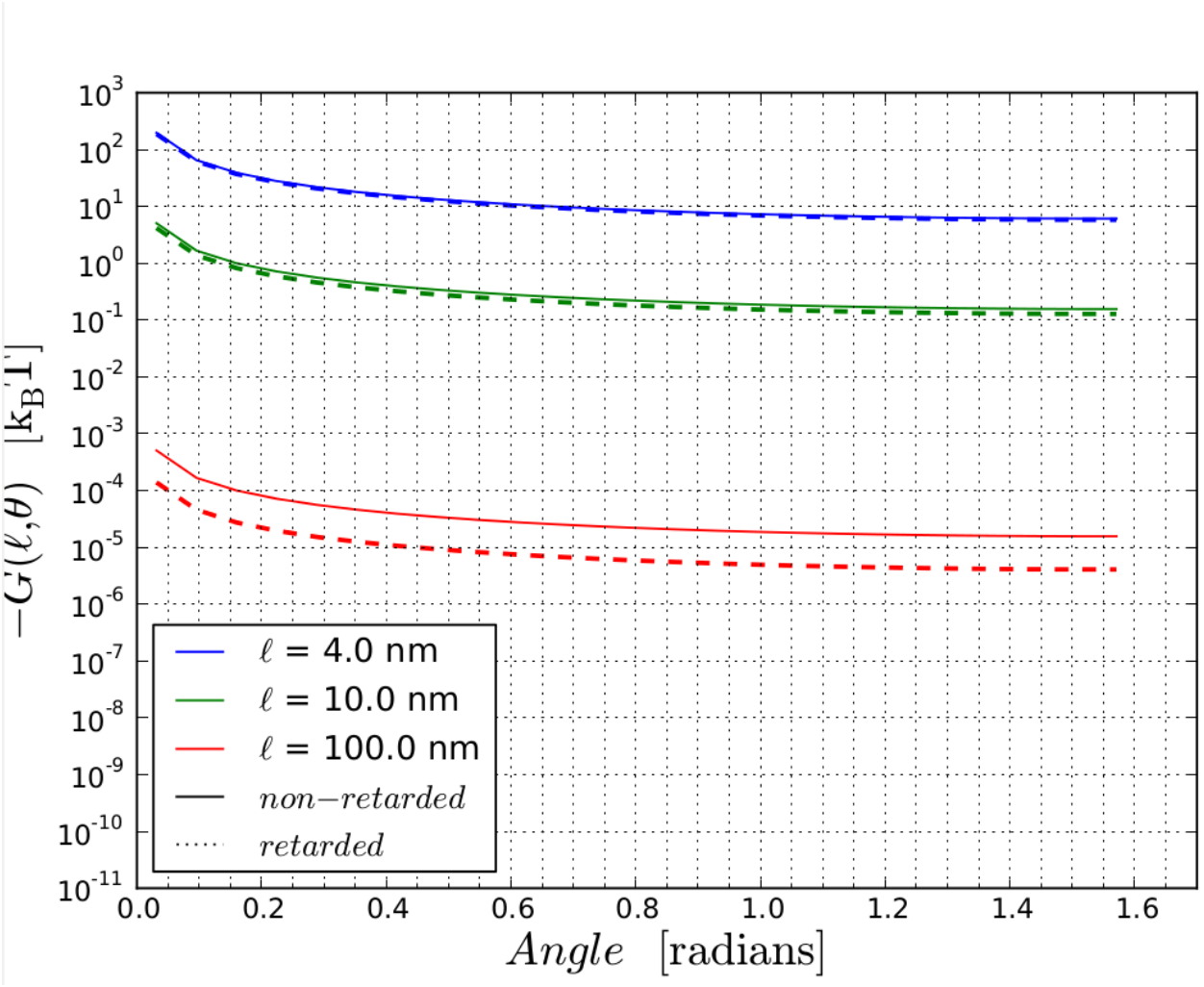

Figure 17: $\mathcal{G}(\theta)$ for [6,5] in water

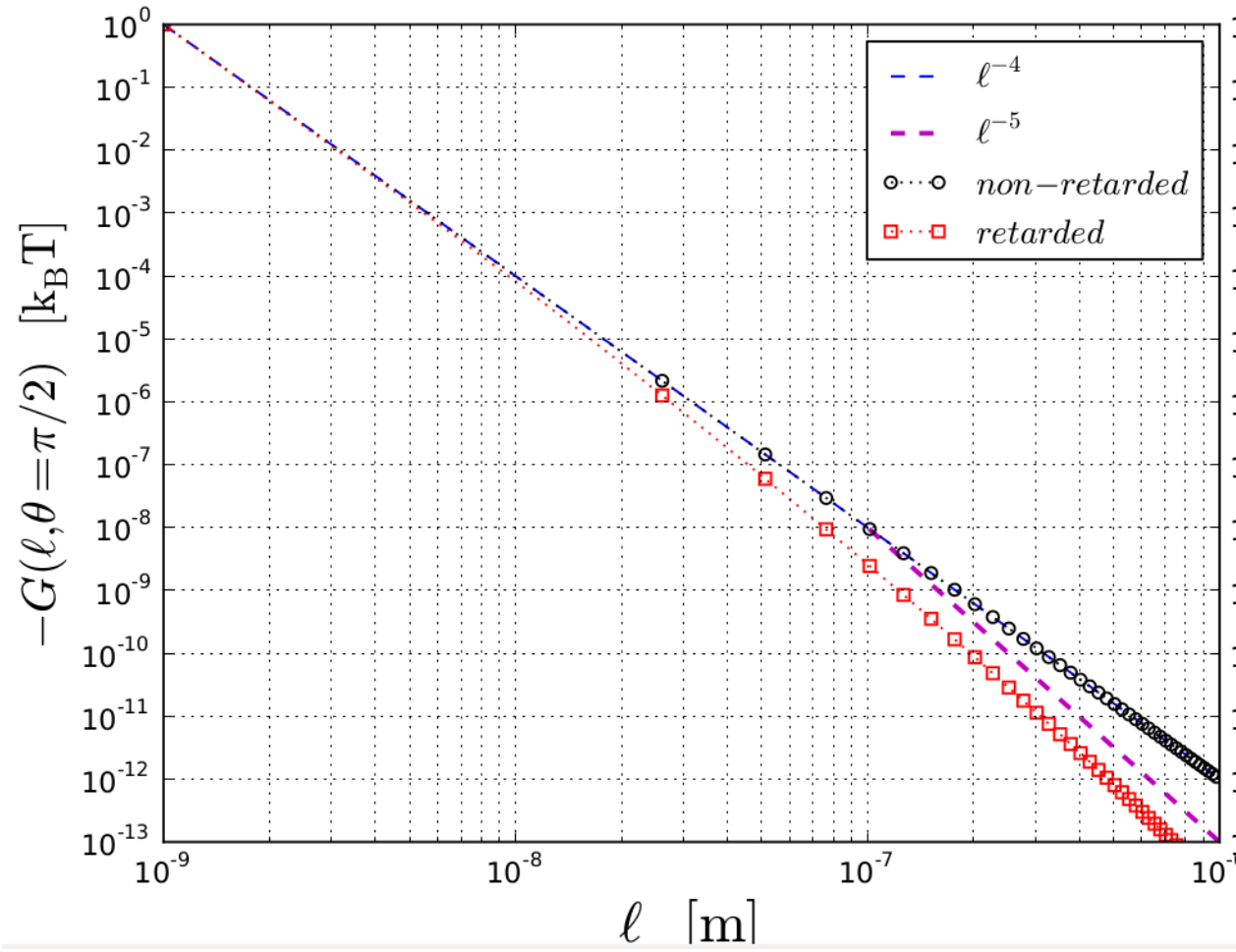

Figure 18: $\mathcal{G}(\ell)$ for [6,5] in water

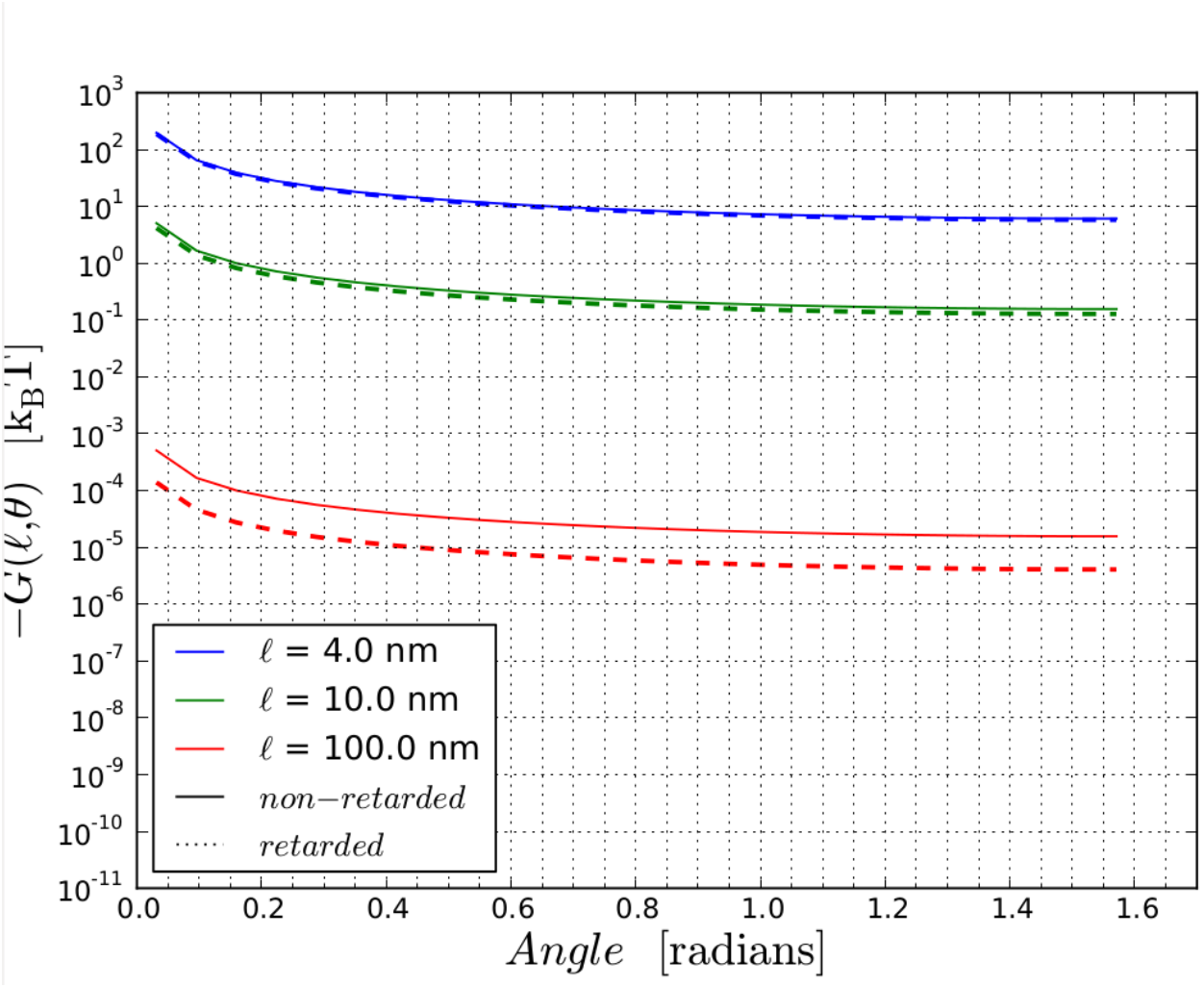

Figure 19: $\mathcal{G}(\theta)$ for [6,5] in water